

Cross-correlation Full Waveform Inversion for Sound Speed Reconstruction in Ultrasound Computed Tomography*

Yue Zhao, Nuomin Zhang, Xin Lu, Yu Yuan, and Yi Shen

Abstract— Ultrasound computed tomography (USCT) is considered to have great potential for breast cancer screening. Compared with the ray based methods, the reconstructed image using full waveform inversion (FWI) methods have higher spatial resolution. However, the results of FWI is difficult to converge to the real value when cycle skipping occurs. In this paper, a cross-correlation full waveform inversion (CC-FWI) is proposed for USCT image reconstruction. In the first stage, the adjoint source is adjusted as the residual of predicted signal and time-shifted measured signal to avoid cycle skipping. In the remaining stage, the FWI with source encoding is employed to accelerate convergence. The simulations are conducted to demonstrate the validity of the proposed algorithm. The root mean squared error (RMSE) of the proposed algorithm is much smaller than that of conventional FWI. The results suggest that CC-FWI is effective in avoiding cycle skipping.

Clinical relevance— New imaging modalities of high resolution, safety to examines for early-stage breast cancer imaging are urgently needed for researching and development. Ultrasound computed tomography (USCT) is supposed to meet the above requirements and it can be potentially deployed in breast scanning.

I. INTRODUCTION

Breast cancer is currently a global public health issue [1]. Ultrasound computed tomography (USCT) is considered as a potential breast imaging method [2]–[4]. USCT system can reconstruct the acoustic reflectivity, sound speed or acoustic attenuation distribution of the breast tissues, and in this study we focus on the reconstruction of the sound speed distribution using USCT.

Recently, the full waveform inversion (FWI) methods, which is traditionally investigated in seismology [5], [6], are proposed for USCT reconstruction in medical imaging [7]–[11]. Thanks to the forward and backward model of FWI method, the resolution of the reconstructed images is higher comparing with the ray based methods. However, since the wave equations need to be solved during reconstruction using FWI, it has two common problems: high computational burden and poor convergence [7].

* This research was partially supported by the Natural Science Foundation of China (62173116) the Postdoctoral Research Funds of Heilongjiang Province (Grant No. LBH-TZ13 and No. LBH-Z15068), postdoctoral initial funding of Heilongjiang Province (No. LBH-Q21097) and Degree Post-graduate Education Reform Project of Harbin Institute of Technology (No. 21MS002).

Yue Zhao, Nuomin Zhang, Yu Yuan and Yi Shen are with the Department of Control Science and Engineering, Harbin Institute of Technology, Harbin 150001, China. (Corresponding author: Nuomin Zhang, 0086-138-4750-1097, 21B904072@stu.hit.edu.cn; yue.zhao@hit.edu.cn; 16B904010@stu.hit.edu.cn; shen@hit.edu.cn)

Xin Lu is with School of Computer Science and Informatics Faculty of Computing, Engineering and Media (CEM), De Montfort University, Leicester, United Kingdom. (xin.lu@dmu.ac.uk)

To decrease the computational burden, the approaches that combines waveform inversion with source encoding were proposed [5], [8], [10]. Zhang *et al.* proposed a source coding approach. To distinguish different sources, random phase is implemented to each source in this method [8]. This method greatly reduces the time of image reconstruction. Wang *et al.* proposed a waveform inversion method with source encoding, which used a random encoding vector to encode the measurement data [10]. This method improves computational efficiency while maintaining high spatial resolution of imaging results.

Beside the high computational burden, the FWI methods has another problem called cycle skipping [6]. This phenomenon is caused by the large difference between the initial model and the real model. Wang *et al.* used the result of ray based methods as the initial model [10]. However, when the sound speed distribution of medium differs greatly from the initial model, the reconstruction result of ray based method is not accurate, and the cycle skipping cannot be completely avoided in this case. Because the cycle skipping is related to the emitting frequency, Bernard *et al.* presented a new FWI method with multi-frequency sources [11]. This method uses a series of sources from low frequency to high frequency to reconstruct the sound speed distribution of the medium. However, this method increases the difficulty and cost of hardware manufacturing.

In this paper, a cross-correlation full waveform inversion (CC-FWI) algorithm is proposed. By calculating the correlation between the measured signal and the predicted signal, the residual of the time-shifted measured signal and the predicted signal is taken as the adjoint source to guide the gradient down from the correct direction and thus, the cycle skipping is avoided. Since source encoding will affect the results of cross-correlation calculation, a two-stage inversion strategy is implemented. The first stage employs CC-FWI. When the correlation between the predicted signal and the measured signal is less than a certain threshold value, the cycle skipping will not happen with this estimated sound speed distribution using FWI algorithm. Then, FWI with source encoding in ref [10] is used to reduce the amount of calculation and accelerate convergence. The simulation results show that the proposed method is effective in avoiding the cycle skipping, which performs much better to conventional FWI method.

The remainder of this paper is organized as follows: the CC-FWI is described in section II; the simulation setups and imaging results are shown in section III and the discussion and conclusion is given in part IV.

II. METHODS

A. USCT Imaging Model

In this study, we consider a circular array of ultrasound transducers surrounding the medium to be imaged, and there are M ultrasound transducers uniformly spaced on the array. The pulse emitted by the m th transducer is $s_m(x, t)$, and it generates an acoustic pressure wavefield noted as $p_m(x, t)$ when it propagates through the medium. If the acoustic absorption and mass density variations are negligible, the propagation of $p_m(x, t)$ in the simulation domain Ω satisfies the acoustic wave equation:

$$\nabla^2 p_m(x, t) - \frac{1}{c^2(x)} \frac{\partial^2}{\partial t^2} p_m(x, t) = s_m(x, t) \quad (1)$$

In general, the expression of $s_m(x, t)$ is:

$$s_m(x, t) = \delta(x - x_m) e^{-\frac{(t-t_0)^2}{2\sigma^2}} \cos(2\pi f t) \quad (2)$$

here f is the emitted frequency. The pressure signal on the circle Γ , the boundary of Ω , is recorded by the transducers as $g_m(x, t)$. The sound speed distribution and measured signal can be expressed as a nonlinear operator R_m , defined as

$$R_m : c(x) \in L^2(\Omega) \longrightarrow g_m(x, t) \in L^2(\Gamma \times (0, T))$$

The USCT reconstruction problem is to solve the nonlinear equations(3):

$$R_m(c) = g_m \quad (3)$$

that is, to estimate the sound speed distribution $c(x)$ from the measured signal $\{g_m(x, t) | m = 0, 1, \dots, M-1\}$.

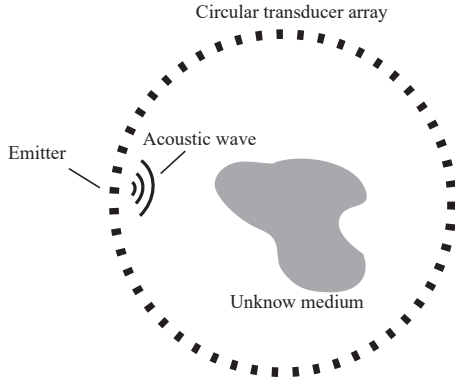


Fig. 1. The USCT setup

B. FWI Algorithm

The traditional FWI method solves the nonlinear equation (3) by minimizing the following numerical optimization problem:

$$\hat{c} = \arg \min_c F(c) \quad (4)$$

here $F(c)$ is the cost function. In general, $F(c)$ is defined as the square of L^2 norms of the data residuals corresponding to measured signal and predicted signal:

$$F(c) = \frac{1}{2} \sum_{m=0}^{M-1} \|R_m(c) - g_m\|^2 \quad (5)$$

The Fréchet derivative of $F(c)$ with respect to c , denoted by J , which can be computed via an adjoint state method as:

$$J = \frac{1}{c^3(x)} \sum_{m=0}^{M-1} \int_0^T q_m(x, T-t) \frac{\partial^2 p_m(x, t)}{\partial t^2} dt \quad (6)$$

here $q_m(x, t)$ is called the adjoint wavefield. It is the solution of the adjoint equation:

$$\nabla^2 q_m(x, t) - \frac{1}{c^2(x)} \frac{\partial^2}{\partial t^2} q_m(x, t) = -\tau_m(x, t) \quad (7)$$

here $\tau_m(x, t) = \overline{g_m}(x, T-t) - g_m(x, T-t)$ is called the adjoint source. $\overline{g_m}(x, t)$ is the predicted signal and $g_m(x, t)$ is the measured signal [10].

In the forward model of FWI method using source encoding, M ultrasound transducers emit ultrasound signals simultaneously. In this condition, the random coding vector is w , the emitted sources and the pressure field can be formulated as:

$$s_w(x, t) = \sum_{m=0}^{M-1} w(m) s_m(x, t) \quad (8)$$

$$p_w(x, t) = \sum_{m=0}^{M-1} w(m) p_m(x, t) \quad (9)$$

The cost function can be reformulated in a stochastic framework as:

$$F_w(c) = E_w \left\{ \frac{1}{2} \|R_w(c) - g_w\|^2 \right\} \quad (10)$$

The Fréchet derivative is computed similarly to the equation(5).

$$\nabla^2 q_w(x, t) - \frac{1}{c^2(x)} \frac{\partial^2}{\partial t^2} q_w(x, t) = -\tau_w(x, t) \quad (11)$$

$$\tau_w(x, t) = \overline{g_w}(x, T-t) - g_w(x, T-t) \quad (12)$$

C. CC-FWI

The reason of cycle skipping is that the travelling time difference between the measured signal and the predicted signal is more than half period. Therefore, time shift strategy is implemented to reduce the travelling time difference between the measured signal and the predicted signal. Thanks to this strategy, the estimated sound speed would not converge to the local minimum value by gradient descent and cycle skipping can be avoided.

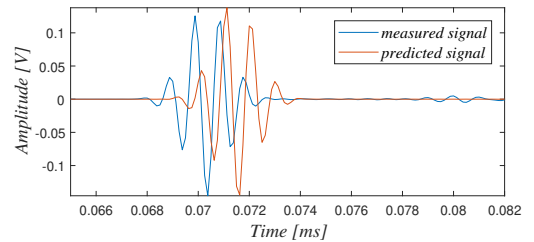


Fig. 2. The measured signal and predicted signal when cycle skipping occurs

The traveling time difference between the measured signal and the predicted signal at the spatial position x is the maximum of cross-correlation, which can be formulated as:

$$d_m(x) = \arg \max_{\tau} \int \overline{g_m(x,t)} g_m(x,t+\tau) dt \quad (13)$$

To avoid cycle skipping, the traveling time difference Δt and the emitted frequency should satisfy the following conditions:

$$|\Delta t| < \frac{0.5}{f} \quad (14)$$

Therefore, the adjoint source $\tau'_m(x,t)$ is adjusted as:

$$\tau'_m(x,t) = \overline{g_m(x,t)} - g_m(x,t + \Delta_m(x)) \quad (15)$$

$\Delta_m(x)$ is a function of traveling time difference $d_m(x)$:

$$\Delta_m(x) = \begin{cases} d_m(x) - \delta, & d_m(x) > \delta \\ 0, & -\delta \leq d_m(x) \leq \delta \\ d_m(x) + \delta, & d_m(x) < -\delta \end{cases} \quad (16)$$

here δ is denoted as a threshold and $0 < \delta < \frac{0.5}{f}$. Then the traveling time difference between $\overline{g_m(x,t)}$ and $g_m(x,t + \Delta_m(x))$ is less than the threshold δ . The calculation of gradient is similar to equation(6). Considering that using the source encoding will affect the calculation of cross-correlation, a two-stage inversion strategy is used. In the first stage, the CC-FWI is employed until the traveling time difference between the predicted signal $\overline{g_m(x,t)}$ and the measured signal $g_m(x,t)$ is less than threshold δ . Then the FWI with source encoding is used to effectively accelerate convergence.

III. SIMULATIONS AND RESULTS

A. Settings of the Simulations

The experiments are implemented in simulations based on the MATLAB R2019b to compare the reconstruction results of different methods. The simulation is operated on a workstation, with a AMD EPYC™ 7742 CPU, 4 NVIDIA A100 GPUs and 512 GB memory. The propagation of acoustic wave in the medium is simulated using numeric solution of wave equation in k-space pseudo-spectral method. Two simulations using simple and complicated digital phantoms are performed to illustrate the effectiveness of the proposed algorithm.

The digital phantoms are designed as show in Fig.3. The field of view of each phantom is $120 \times 120 \text{ mm}^2$ and the sound speed of the background is 1500 m/s . A circular transducer array of diameter 100 mm with 256 elements uniformly distributed on it is used to emit and receive the ultrasound signals. In phantom 1, the emitted frequency is 1MHz and the field of view is divided into 320×320 grids. A circular medium with the diameter of 50 mm is in the center and its sound speed is 1550 m/s . In phantom 2, the emitted frequency is 1.5MHz and the field of view is divided into 480×480 grids. The medium of diameter 60mm in the center, is composed of 8 structures representing adipose tissues, parenchymal breast tissues, cysts, benign tumors, and

malignant tumors. The corresponding sound speed are listed in Table I.

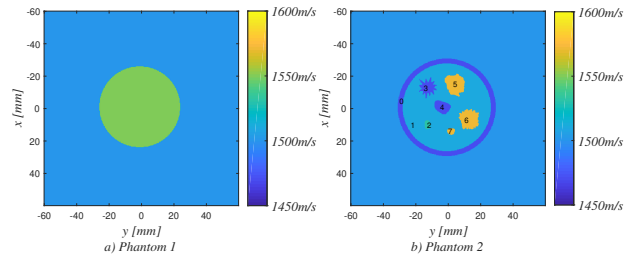


Fig. 3. Digital phantoms used in the simulations

TABLE I
PARAMETERS OF THE PHANTOM 2

Region index	Tissue type	Sound speed (m/s)
0	Adipose	1470
1	Parenchyma	1510
2	Cyst	1530
3	Benign tumor	1470
4	Benign tumor	1470
5	Malignant tumor	1570
6	Malignant tumor	1570
7	Malignant tumor	1570

Firstly, we employ 300 iterations of FWI with source encoding to reconstruct the sound speed distribution. Then CC-FWI is employed to compare the results. In the first stage of CC-FWI, the threshold δ is set as $\frac{0.25}{f}$. In the second stage, the number of iterations is 100.

B. Results

The imaging results of the two phantom using FWI and the proposed algorithm are shown in Fig.4 and Fig.5.

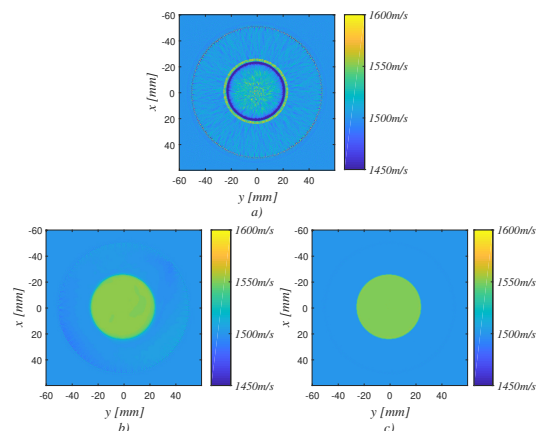


Fig. 4. Reconstructed results of phantom 1: a) the result of conventional FWI, b) the result of the first stage of the CC-FWI, c) the final result of the CC-FWI

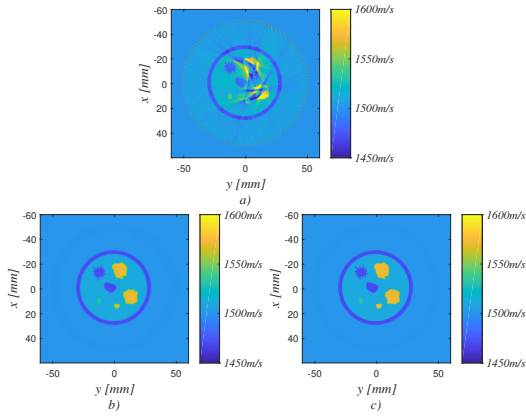


Fig. 5. Reconstructed results of phantom 1: a) the result of conventional FWI, b) the result of the first stage of the CC-FWI, c) the final result of the CC-FWI

It can be seen from reconstructed results that compared with conventional FWI, the algorithm proposed has a great improvement in reconstruction result of USCT. Due to the cycle skipping, the result of conventional FWI has a terrible error with the phantom and it is not credible. However, the CC-FWI method can reconstruct the sound speed of medium well. In the first stage, when the traveling time difference is less than the threshold, the discrepancy between the reconstructed sound speed and the phantom is smaller than the result of conventional FWI. After the calculation of second stage, the reconstructed sound speed is close to the phantom. The result of the phantom 2 shows that, although some region can be reconstructed using conventional FWI, the region like 5. 6. 7 of Fig.3 b) are reconstructed incorrectly with streak artifacts because the difference between the initial model and real value is so large that it leads to cycle skipping. However, the sound speed in the medium can be reconstructed properly using the CC-FWI.

In order to further quantitatively compare the reconstruction results, the root mean squared error (RMSE) is chosen as the evaluation criterion.

$$RMSE = \sqrt{\frac{\sum_{i=1}^N (y(i) - y'(i))^2}{N}} \quad (17)$$

here y is the standard image of N grids, and y' is the reconstructed result of y . As shown in Fig.6, the RMSEs with the proposed algorithm is $10m/s$ less than that of the conventional FWI. This confirms the effective of the proposed algorithm in the case of cycle skipping.

IV. DISCUSSIONS AND CONCLUSIONS

In this paper, the CC-FWI is proposed to reduce the cycle skipping phenomenon of the traditional FWI algorithm. Cross-correlation is calculated to reduce the travelling time difference between the measured signal and predicted signal. After the traveling time difference satisfies the conditions, FWI with source encoding is employed to accelerate convergence. In order to prove the validity of the algorithm, two

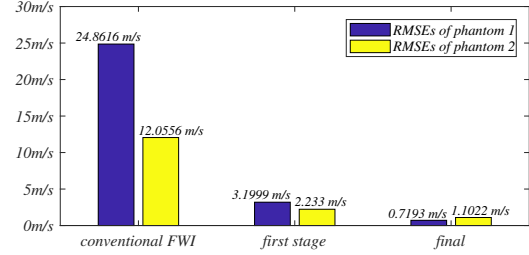


Fig. 6. The RMSEs of reconstruction results

simulation experiments was conducted. Experimental results show that the error of the the CC-FWI method is less than that of the conventional FWI method. Therefore, the CC-FWI is certificated to be an effective imaging algorithm in USCT.

Since the two-stage inversion strategy increases the calculated amount. in further work, we will find a better way to combine the CC-FWI with source encoding and validate this method for in vivo imaging applications. Reconstruction of more complex phantom may be explored.

REFERENCES

- [1] R. W. Carlson, D. C. Allred, B. O. Anderson, H. J. Burstein, W. B. Carter, S. B. Edge, J. K. Erban, W. B. Farrar, L. J. Goldstein, W. J. Gradishar et al., "Breast cancer," Journal of the National Comprehensive Cancer Network, vol. 7, no. 2, pp. 122–192, 2009.
- [2] N. Duric, P. Littrup, L. Poulou, A. Babkin, R. Pevzner, E. Holsapple, O. Rama, and C. Glide, "Detection of breast cancer with ultrasound tomography: first results with the computed ultrasound risk evaluation (cure) prototype," Medical Physics, vol. 34, no. 2, 2007.
- [3] C. Li, N. Duric, P. Littrup, and L. Huang, "In vivo breast sound-speed imaging with ultrasound tomography," Ultrasound in medicine biology, vol. 35, no. 10, pp. 1615–1628, 2009.
- [4] N. Duric, P. Littrup, O. Roy, S. Schmidt, C. Li, and L. Beyknight, "Breast imaging with ultrasound tomography: Initial results with softvue," IEEE, 2013.
- [5] J. R. Krebs, J. E. Anderson, D. Hinkley, R. Neelamani, S. Lee, A. Baumstein, and M.-D. Lacasse, "Fast full-wavefield seismic inversion using encoded sources," Geophysics, vol. 74, no. 6, pp. WCC177–WCC188, 2009.
- [6] J. Virieux and S. Operto, "An overview of full-waveform inversion in exploration geophysics," Geophysics, vol. 74, no. 6, pp. WCC1–WCC26, 2009.
- [7] O. Roy, I. Jovanović, A. Hormati, R. Parhizkar, and M. Vetterli, "Sound speed estimation using wave-based ultrasound tomography: theory and gpu implementation," in Medical Imaging 2010: Ultrasonic Imaging, Tomography, and Therapy, vol. 7629. International Society for Optics and Photonics, 2010, p. 76290J.
- [8] Z. Zhang, L. Huang, and Y. Lin, "Efficient implementation of ultrasound waveform tomography using source encoding," in Medical Imaging 2012: Ultrasonic Imaging, Tomography, and Therapy, vol. 8320. International Society for Optics and Photonics, 2012, p. 832003.
- [9] J. Wiskin, D. Borup, S. Johnson, and M. Berggren, "Non-linear inverse scattering: high resolution quantitative breast tissue tomography," The Journal of the Acoustical Society of America, vol. 131, no. 5, pp. 3802–3813, 2012.
- [10] K. Wang, T. Matthews, F. Anis, C. Li, N. Duric, and M. Anastasio, "Waveform inversion with source encoding for breast sound speed reconstruction in ultrasound computed tomography," IEEE Transactions on Ultrasonics Ferroelectrics Frequency Control, vol. 62, no. 3, pp. 475–93, 2015.
- [11] S. Bernard, V. Monteiller, D. Komatitsch, and P. Lasaygues, "Ultrasonic computed tomography based on full-waveform inversion for bone quantitative imaging," Physics in Medicine Biology, vol. 62, no. 17, p. 7011, 2017.